Synthesis and Spectroscopic Characterization of Octaacetic Acid Tetraphenylporphyrins

ARTICLE *in* INORGANIC CHEMISTRY · DECEMBER 1994

Impact Factor: 4.76 · DOI: 10.1021/ic00104a016

Synthesis and Spectroscopic Characterization of Octaacetic Acid Tetraphenylporphyrins

Michiko Miura,*,† Sabir A. Majumder,‡,§ J. David Hobbs,‡ Mark W. Renner,‖ Lars R. Furenlid,⊥ and John A. Shelnutt*,‡,§

Medical Department, Department of Applied Science, and National Synchrotron Light Source, Brookhaven National Laboratory, Upton, New York 11973, Fuel Science Department, Sandia National Laboratories, Albuquerque, New Mexico 87185-0710, and Department of Chemistry, University of New Mexico, Albuquerque, New Mexico 87131

Received December 22, 1993⊗

Members of a new class of water-soluble, nonplanar porphyrins based on 5,10,15,20-tetraphenylporpyrin-2,3,7,8,-12,13,17,18-octaacetic acid (OAATPPs) have been synthesized, and their physical and chemical properties as well as their interactions with complexing agents have been investigated using UV−visible absorption, EXAFS, nuclear magnetic resonance and resonance Raman spectroscopies. Red shifts of 19−36 nm in the major absorption bands are noted for Ni derivatives of OAATPP and its octamethyl ester (OME), *meso*-tetrakis(*p*-nitrophenyl)-porphyrinoctaacetic acid octamethyl ester, and octakis(hydroxyethyl)tetraphenylporphyrin relative to nickel tetraphenylporphyrin. These red shifts are indicative of a high degree of nonplanarity. The short Ni−N distances of 1.92(2) Å for NiOAATPP-OME and 1.89(2) Å for NiOAATNPP-OME from EXAFS experiments corroborate the nonplanar nature of these porphyrins. The decreased ring current effect and temperature-dependent NMR measurements also confirm that the porphyrins are nonplanar in solution. Resonance Raman studies also indicate nonplanar conformations for NiOAATPP and its derivatives by the characteristic downshifts in the frequencies of the structure-sensitive marker lines. At low pH (<3) or in 4.5 M NaCl, conditions under which planar octaacid porphyrins like nickel uroporphyrin form $\pi-\pi$ aggregates that give small characteristic upshifts in the structure-sensitive Raman lines, NiOAATPP shows no significant changes in either the absorption or the Raman spectra. The $\pi-\pi$ aggregates formed by planar Ni uroporphyrin do not form for NiOAATPP most likely because of the steric difficulty in stacking the highly nonplanar and sterically hindered OAATPPs. Finally, the affinity for axially coordinated nitrogenous bases is decreased by nonplanarity and increased by electron-withdrawing peripheral substituents.

Introduction

There is current interest in the chemical and physical properties of nonplanar porphyrins and hydroporphyrins. In particular, nonplanar distortions of the macrocycle which result from steric interactions among the peripheral substituents have been investigated in order to understand the functional consequences of similar distortions observed for the tetrapyrrole derivatives in various proteins.[1−3] These nonplanar structural distortions include the ruffled (*ruf*) and/or saddle (*sad*) structures of the porphyrin macrocycle defined by Scheidt and Lee.[4] Nonplanar structural changes in the macrocycle that are caused by the protein environment are believed to be important in the function of photosynthetic reaction centers,[5] methylreductase[6,7] and heme proteins.[8,9] These nonplanar distortions are expected to influence chemical processes such as the binding and release of axial ligands, redox properties of the porphyrin and the central metal ion, and electron-transport properties.[10−13]

An interesting example of the possible relevance of nonplanar distortions of the porphyrin prosthetic group has been reported for *c*-type cytochromes.[8] An analysis of high-resolution X-ray crystal structures for cytochromes *c* isolated from various species reveals the presence of a conserved nonplanar distortion of the hemes that is induced primarily through covalent linkages between the 2- and 4-vinyl substituents of protoheme and two cysteine residues of the protein. Further, this heme distortion must be even more highly conserved than is indicated by the

* To whom correspondence should be addressed.
† Medical Department, Brookhaven National Laboratory.
‡ Sandia National Laboratories.
§ University of New Mexico.
‖ Department of Applied Science, Brookhaven National Laboratory.
⊥ National Synchrotron Light Source, Brookhaven National Laboratory.
⊗ Abstract published in *Advance ACS Abstracts,* November 15, 1994.

(1) Barkigia, K. M.; Berber, M. D.; Fajer, J.; Medforth, C. J.; Renner, M. W.; Smith, K. M. *J. Am. Chem. Soc.* **1990**, *112*, 8851.
(2) Sparks, L. D.; Medforth, C. J.; Park, M.-S.; Chamberlain, J. R.; Ondrias, M. R.; Senge, M. O.; Smith, K. M.; Shelnutt, J. A. *J. Am. Chem. Soc.* **1993**, *115*, 581.
(3) (a) Shelnutt, J. A.; Medforth, C. J.; Berber, M. D.; Barkigia, K. M.; Smith, K. M. *J. Am. Chem. Soc.* **1991**, *113*, 4077. (b) Medforth, C. J.; Senge, M. O.; Smith, K. M.; Sparks, L. D.; Shelnutt, J. A. *J. Am. Chem. Soc.* **1992**, *114*, 9859.
(4) Scheidt, W. R.; Lee, Y. J. *Struct. Bonding* **1987**, *64*, 1.
(5) Deisenhofer, J.; Michel, H. *Science* **1989**, *245*, 1463.
(6) (a) Eschenmoser, A. *Ann. N.Y. Acad. Sci.* **1986**, *471*, 108. (b) Furenlid, L. R.; Renner, M. W.; Smith, K. M.; Fajer, J. *J. Am. Chem. Soc.* **1990**, *112*, 1634. (c) Furenlid, L. R.; Renner, M. W.; Fajer, J. *J. Am. Chem. Soc.* **1990**, *112*, 8987.
(7) (a) Shiemke, A. K.; Scott, R. A.; Shelnutt, J. A. *J. Am. Chem. Soc.* **1988**, *110*, 1645. (b) Schiemke, A. K.; Shelnutt, J. A.; Scott, R. A. *J. Biol. Chem.* **1989**, *264*, 11236. (c) Shiemke, A. K.; Kaplan, W. A.; Hamilton, C. L.; Shelnutt, J. A.; Scott, R. A. *J. Biol. Chem.* **1989**, *264*, 7276. (d) Shelnutt, J. A. *J. Am. Chem. Soc.* **1987**, *109*, 4169. (e) Crawford, B. A.; Findsen, E. W.; Ondrias, M. R.; Shelnutt, J. A. *Inorg. Chem.* **1988**, *27*, 1842. (f) Shelnutt, J. A. *J. Phys. Chem.* **1989**, *93*, 6283.
(8) Hobbs, J. D.; Shelnutt, J. A. *J. Protein Chem.* **1994**, in press.
(9) Ladner, R. C.; Heidner, E. J.; Perutz, M. F. *J. Mol. Biol.* **1977**, *114*, 385.
(10) Barkigia, K. M.; Chantranupong, L.; Smith, K. M.; Fajer, J. *J. Am. Chem. Soc.* **1988**, *110*, 7566.
(11) (a) Kratky, C.; Waditschatka, R.; Angst, C.; Johansen, J.; Plaquerent, J. C.; Schreiber, J.; Eschenmoser, A. *Helv. Chem. Acta* **1982**, *68*, 1312. (b) Waditschatka, R.; Kratky, C.; Juan, B.; Heinzer, J.; Eschenmoser, A. *J. Chem. Soc., Chem. Commun.* **1985**, 1604.
(12) Geno, M. K.; Halpern, J. *J. Am. Chem. Soc.* **1987**, *109*, 1238.
(13) Hobbs, J. D.; Majumder, S. A.; Luo, L.; Sickelsmith, G. A.; Quirke, J. M. E.; Medforth, C. J.; Shelnutt, J. A. *J. Am. Chem. Soc.* **1994**, *116*, 3261.

0020-1669/94/1333-6078$04.50/0

X-ray structures because resonance Raman spectra of cytochromes *c* from a large number and variety of species show only small differences in the frequencies of the structure-sensitive Raman lines.[14] Moreover, a recent resonance Raman study of metal-substituted octaethylporphyrins (OEPs) and 5-nitrooctaethylporphyrins (5-NO_2OEPs) indicates that nonplanar distortions in porphyrins that contain metals like iron, which give porphinato core sizes of *ca.* 2.00 Å or greater, can occur only as a result of a perturbation brought about by the macrocycle's environment.[15] Thus, for the case of cytochromes *c*, the conserved nonplanar distortion is maintained by the protein at the expense of significant energy. This observation suggests a possible functional role for modifications of heme planarity that occur as a result of changes in metal oxidation state upon electron transfer or that occur as a result of changes in the tertiary structure of the protein upon binding to physiological reaction partners.

Nickel porphyrins are attractive model systems for investigating the role of porphyrin deformation in the function of biological systems. Their response to different environmental perturbations are simplified compared to the Fe porphyrins because they typically exist in only the Ni(II) oxidation state, in only two spin states (high ($S = 1$) and low ($S = 0$)), and in coordination numbers of 4 (low spin), 5 (high spin), and 6 (high spin) with σ-donating axial ligands.[16] Further, the tendency toward nonplanar distortions is enhanced for low-spin nickel because the optimum unconstrained Ni−N bond distance (1.85 Å) is smaller than the optimum porphyrin metal−nitrogen bond distance (≈2.00 Å) for a planar porphyrin. As a result of its small size, nickel prefers a distorted macrocycle conformation. Nonplanar distortion allows the pyrrole nitrogens to approach the nickel ion more closely than for a planar macrocycle. The distortion disturbs the π-conjugation of the macrocycle resulting in a red-shifted absorption spectrum.[2,3] The distortion also significantly affects the porphyrin ring vibrational modes inducing several structure-sensitive Raman marker lines to shift toward low frequency. Also, the nonplanar macrocycle distortion of Ni porphyrins causes a decrease in axial ligand affinity when compared to the case of planar Ni porphyrins because the distorted porphyrin is more coordinatively saturated by the closer equatorial ligands of its contracted core.

Herein, we present the syntheses and physical properties of tetraphenylporphyrins possessing eight acetic acid groups at the pyrrole β positions and the corresponding methyl esters of these tetraphenylporphyrin derivatives. Properties of this new class of porphyrins based on 5,10,15,20-tetraphenylporphyrin-2,3,7,8,-12,13,17,18-octaacetic acid (OAATPPs) were determined using UV−visible absorption, EXAFS, nuclear magnetic resonance and resonance Raman spectroscopies. The deprotonated free acid form of each of these porphyrins is soluble in water. The octaacetic acid tetraphenylporphyrins are found to be highly nonplanar as a result of the steric crowding of the twelve peripheral substituents. The only other reports[17,18] on the synthesis of water-soluble porphyrins that are significantly distorted from planarity include octabromo- and octachloro-*meso*-tetrakis(sulfonatophenyl)porphyrins and their manganese and iron derivatives. However, these octahalogenated tetraphenylporphyrin derivatives are less sterically hindered in their interactions (with other molecules) than the OAATPP derivatives described here (unpublished molecular mechanics results). Specifically, we have investigated the effects of nonplanarity on the physical properties of Ni(II) derivatives of tetraphenylporphyrinoctaacetic acid (**4**: OAATPP), its octamethyl ester (**3**: OAATPP-OME), octakis(hydroxyethyl)tetraphenylporphyrin (**5**: OHETPP), and tetrakis(*p*-nitrophenyl)porphyrinoctaacetic acid octamethyl ester (**6**: OAATNPP-OME). The structures of these new porphyrins are shown in Figure 1. Distinct chemical properties are expected for these nickel porphyrins because of their nonplanarity and because of the differing electronic effects of the pyrrole substituents. Both the acetic acid ester substituent and the protonated acetic acid substituent are more electron-withdrawing than the alkyl, hydroxyethyl and deprotonated acetic acid substituents. Also, the *p*-nitrophenyl meso-substituent is more electron-withdrawing than the unsubstituted phenyl group. Thus, these electronic effects must be considered in combination with conformational influences when correlating differences in spectral and chemical properties of these new dodecasubstituted porphyrins.

We have also used resonance Raman and UV−visible absorption spectroscopies to investigate the $\pi-\pi$ aggregation behavior of nonplanar NiOAATPP in aqueous solution. The weak interactions occurring in aggregates and $\pi-\pi$ complexes of these porphyrins are analogous to the interactions between the macrocycle and amino acid residues lining the porphyrin binding site in a protein. The aggregation properties of NiOAATPP are compared to the results for metallouroporphyrins (MUroPs), for which the weak interactions resulting from $\pi-\pi$ self-aggregation[19−23] and $\pi-\pi$ complex formation[22−25] have been investigated in detail. The MUroPs are convenient for such studies because they can exist in both aggregated and unaggregated forms. The lack of appreciable aggregation of MUroPs at high pH (pH > 8) or at moderate concentrations (<0.01 M) is attributed to electrostatic repulsion of the eight ionized acetic and propionic acid substituents at the β-carbon positions of the pyrrole rings. However, the uroporphyrins aggregate at low pH or upon addition of salt (>1 M) because of shielding of the charges on the carboxylate groups. Like uroporphyrin, OAATPP contains eight ionizable acetic acid groups at the β positions of the pyrrole rings, and might be expected to show similar aggregation behavior. However, as a result of the nonplanar distortion and resulting steric constraints on intermolecular interactions, we find that $\pi-\pi$ aggregates do not form either at low pH or at high ionic strength.

(14) (a) Shelnutt, J. A.; Rousseau, D. L.; Dethmers, J. K.; Margoliash, E. *Biochemistry* **1981**, *20*, 6485. (b) Shelnutt, J. A.; Rousseau, D. L.; Dethmers, J. K.; Margoliash, E. *Proc. Natl. Acad. Sci. U.S.A.* **1979**, *76*, 3865.
(15) Anderson, K. K.; Hobbs, J. D.; Luo, L.; Stanley, K. D.; Quirke, J. M. E.; Shelnutt, J. A. *J. Am. Chem. Soc.* **1993**, *115*, 12346.
(16) (a) Shelnutt, J. A.; Altson, K.; Ho, J.-Y.; Yu, N.-T.; Yamamoto, T.; Rifkind, J. M. *Biochemistry* **1986**, *25*, 620. (b) Findsen, E. W.; Alston, K.; Shelnutt, J. A.; Ondrias, M. R. *J. Am. Chem. Soc.* **1986**, *108*, 4009. (c) Findsen, E. W.; Shelnutt, J. A.; Ondrias, M. R. *J. Phys. Chem.* **1988**, *92*, 307. (d) Shelnutt, J. A.; Findsen, E. W.; Ondrias, M. R.; Alston, K. In *Metal Complexes in Fossil Fuels*; Filby, R. H., Branthaver, J. F., Eds.; ACS Symposium Series 344; American Chemical Society: Washington, DC, 1987; Chapter 24. (e) Shelnutt, J. A.; Alston, K.; Findsen, E. W.; Ondrias, M. R.; Rifkind, J. M. In *Porphyrins: Excited States and Dynamics*; Gouterman, M., Rentzepis, P. M., Straub, K. D., Eds.; ACS Symposium Series 321; American Chemical Society: Washington, DC, 1986; Chapter 16.
(17) Hoffmann, P.; Labat, G.; Robert, A.; Meunier, B. *Tetrahedron Lett.* **1990**, *31*, 1991.
(18) Hoffmann, P.; Robert, A.; Meunier, B. *Bull. Soc. Chim. Fr.* **1992**, *129*, 85.
(19) Blumberg, W. E.; Peisach, J. *J. Biol. Chem.* **1965**, *240*, 860.
(20) Shelnutt, J. A.; Dobry, M. M.; Satterlee, J. D. *J. Phys. Chem.* **1984**, *88*, 4980.
(21) Shelnutt, J. A. *J. Phys. Chem.* **1984**, *88*, 4988.
(22) Shelnutt, J. A. *J. Phys. Chem.* **1984**, *88*, 6121.
(23) Alden, R. G.; Ondrias, M. R.; Shelnutt, J. A. *J. Am. Chem. Soc.* **1990**, *112*, 691.
(24) Mauzerall, D. *Biochemistry* **1965**, *4*, 1801.
(25) Shelnutt, J. A. *J. Am. Chem. Soc.* **1983**, *105*, 7179.

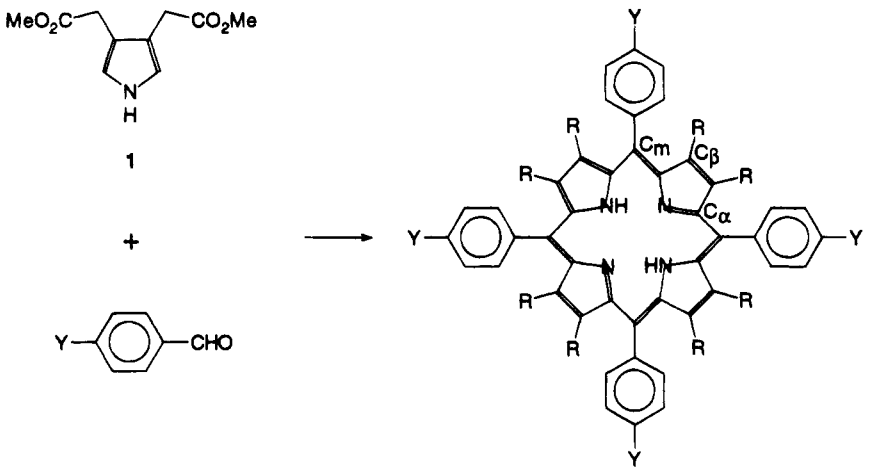

2, Y = H,	R = CH_2CH_3	OETPP
3, Y = H,	R = $CH_2CO_2CH_3$	OAATPP-OME
4, Y = H,	R = CH_2CO_2H	OAATPP
5, Y = H,	R = CH_2CH_2OH	OHETPP
6, Y = NO_2	R = $CH_2CO_2CH_3$	OAATNPP-OME

Figure 1. Structures of pyrrole-3,4-diacetic acid dimethyl ester (**1**) and various planar and nonplanar nickel porphyrins: OETPP (**2**), OAATPP-OME (**3**), OAATPP (**4**), OHETPP (**5**), OAATNP-OME (**6**).

Materials and Methods

Preparation of Ni3. Pyrrole-3,4-diacetic acid dimethyl ester, **1**, was synthesized according to Chiusoli *et al.*[26] and then treated with benzaldehyde under Lindsey's cyclization conditions[27] using $BF_3{\cdot}Et_2O$ as catalyst and dichlorodicyanobenzoquinone as oxidant to yield the porphyrin dication H_4OAATPP-OME, **$H_4$3** (Figure 1) (UV−visible (CH_2Cl_2) λ_{max}, nm: 473, 701). Without further purification the evaporated residue was treated with $Ni(OAc)_2/CHCl_3$ at room temperature and the resultant NiOAATPP-OME, **Ni3**, was purified by preparative TLC (Analtech, Inc.) on silica with 5% acetone/CH_2Cl_2. Recrystallization in CH_2Cl_2/petroleum ether afforded **Ni3** in 12.5% yield from **1**. ^{1}H-NMR ($CDCl_3$): δ 7.92−7.95 (m, 8H Ar *o*-H), 7.59−7.68 (m, 12H, Ar *m*-, *p*-H), 3.33 (s, 24H, OCH_3), 3.25 (s, 16H, CH_2). ^{13}C-NMR (CD_3OD): δ 172.4, 145.7, 139.8, 138.9, 129.9, 129.0, 118.9, 52.0, 33.2. IR ($CHCl_3$): 1738 cm^{-1} (C=O). UV-visible (CH_2Cl_2) λ_{max}, nm ($10^{-3}\epsilon$): 436 (231), 555 (16.2), 568 (8.1). Anal. Calcd for $C_{68}H_{60}N_4O_{16}Ni{\cdot}H_2O$: C, 63.81; H, 5.04; N, 4.38. Found: C, 63.81; H, 5.09; N, 4.30.

Preparation of Ni4. The octacarboxylate NiOAATPP was synthesized by saponification of the ester groups in **Ni3** using KOH/MeOH at reflux overnight. The evaporated residue was purified by ion exchange chromatography (Dowex 50X8-100 resin, H form; 1:1 MeOH/H_2O eluent). ^{1}H-NMR (acetone-d_4): 7.91−7.94 (m, 8H, Ar *o*-H), 7.72−7.75 (m, 4H, Ar *p*-H), 7.63−7.68 (m, 8H, Ar *m*-H), 3.30 (s, 16H, CH_2). UV−visible (0.1 M KOH) λ_{max}, nm: 432, 548, 582.

Preparation of Ni5. Porphyrin **Ni3** was treated with $LiAlH_4$ in THF[28] to yield NiOHETPP after purification with preparative TLC (5% MeOH/CH_2Cl_2). ^{1}H-NMR (CD_3OD): δ 7.98−8.01 (m, 8H, Ar *o*-H), 7.70−7.73 (m, 12H, Ar *m*,*p*-H), 3.03, 2.74−2.88, 2.12−2.27 (32H, CH_2-CH_2). ^{13}C-NMR (CD_3OD): δ 147.4, 142.9, 139.7, 135.4, 130.2, 129.0, 119.0, 64.2. UV−visible (CH_2Cl_2) λ_{max}, nm ($10^{-3}\epsilon$): 436 (113), 555 (8.8), 590 (6.4). FAB MS (*m/e*): 1023 (M^+ + H).

Preparation of Fe3. The Fe(III) Cl porphyrin was synthesized from **$H_4$3** (purified by preparative TLC) using $FeCl_2{\cdot}4H_2O$/DMF and was purified by chromatography (Brockman grade III alumina, 0.5% MeOH/CH_2Cl_2).[2] ^{1}H-NMR ($CDCl_3$), δ: 43.6, 42.0, 33.0, 25.8 (s, CH_2); 13.9 (s, Ar *m*-H); 7.9, 7.8 (m, Ar *o*-H); 6.3 (s, Ar *p*-H). UV−visible (CH_2Cl_2) λ_{max}, nm: 390, 444.

Preparation of Ni6. The *p*-nitrophenyl analog was synthesized as was **Ni3** except that *p*-nitrobenzaldehyde was used for the cyclization. ^{1}H-NMR ($CDCl_3$), δ: 8.52, 8.17 (AB quartet, 16H, Ar H, J = 8.8 Hz); 3.39 (s, 24H, OCH_3); 3.22 (s, 16H, CH_2). UV−visible (CH_2Cl_2) λ_{max}, nm ($10^{-3}\epsilon$): 450 (143), 560 (14.4), 600 (8.8). Anal. Calcd for $C_{68}H_{56}N_8O_{24}Ni$: C, 57.20; H, 3.95; N, 7.85. Found C, 57.29; H, 4.19; N, 7.46.

All chemicals and solvents (packaged in Sure/Seal bottles for moisture-sensitive reactions) were purchased from Aldrich Chemical and used without further purification. Ligand-binding and aggregation studies were carried out according to published procedures.[20,22]

Spectroscopic Methods. ^{1}H- and ^{13}C-NMR were run on a Bruker AM-300 spectrometer. Mass spectra were recorded on a Kratos MS 890 instrument equipped with a Sattlefield FAB gun using a nitrobenzyl alcohol matrix. UV−visible spectra were obtained with either a Beckman DU-8 spectrophotometer or a Hewlett Packard HP 8452A diode array spectrophotometer. Elemental analyses were carried out by Galbraith Laboratories, Inc. (Knoxville, TN).

Resonance Raman spectra were obtained at room temperature using a dual-channel Raman spectrometer described previously.[29] Peak positions for the Raman lines were determined from the fast-Fourier-transform smoothed spectra and corrected relative to the Raman lines of NiOEP in methylene chloride.[30] Approximately 60 mW of either the 406.7-nm or the 413.1-nm laser excitation from a krypton ion laser (Coherent) was used to irradiate the samples contained in a dual-compartment rotating cell. The scattered light from the two samples was collected at 90° to the direction of propagation and polarization of the exciting laser light. The scattered light was analyzed (SPEX 1401 double monochromator), detected by a cooled (−20 °C) Hamamatsu R928P photomultiplier tube, and signals from the two samples were separated electronically. Rotation of the sample cell at 50 Hz enabled

(26) Chiusoli, G. P.; Costa, M.; Reverberi, S. *Synthesis* **1989**, 262.
(27) Lindsey, J. S.; Schreiman, I. C.; Hsu, H. C.; Kearney, P. C.; Marguerettaz, A. M. *J. Org. Chem.* **1987**, *52*, 827.
(28) Smith, K. M.; Eivazi, F.; Martynenko, Z. *J. Org. Chem.* **1981**, *46*, 2189−2193.
(29) Shelnutt, J. A. *J. Phys. Chem.* **1983**, *87*, 605.
(30) (a) Li, X.-Y.; Czernuszewicz, R. S.; Kincaid, J. R.; Stein, P.; Spiro, T. G. *J. Phys. Chem.* **1990**, *94*, 47. (b) Li, X.-Y.; Czernuszewicz, R. S.; Kincaid, J. R.; Stein, P.; Spiro, T. G. *J. Phys. Chem.* **1990**, *94*, 31.

the samples to be probed alternately and also prevented local heating of the samples. Each of the Raman spectra is the sum of 5−10 scans. Spectral resolution was 4 cm^{-1}. Sample integrity was checked periodically during the Raman experiment by examining individual scans. Also, UV−visible absorption spectra were obtained before and after the Raman experiments. The individual Raman lines were subsequently decomposed using Lorentzian line shapes and a least-squares fitting procedure with a sloped, linear baseline to extract the positions, heights, and line widths of individual bands.

X-ray absorption spectra were measured at beam lines X-10C and X-11C at the National Synchrotron Light Source. The Ni^{II}OAATPP-OME sample was prepared as a 5 mM solution in 2-methyltetrahydrofuran using glass cells of published design[31] and the NiOAATNPP-OME sample was prepared as a fine powder on tape. The samples were measured in fluorescence mode at room temperature. Data were collected in 20 min scans to yield a minimum of 10^6 counts of signal at the Ni K-edge. The absolute energy position was calibrated with a Ni metal foil and no changes in energy scale were noted over the course of the experiment.

The data was analyzed with the MacXAFS EXAFS analysis package. The EXAFS oscillations were isolated with standard methods:[32,33] linear extrapolation and subtraction of a pre-edge bulk-absorption contribution, normalization of the edge step, interpolation onto a photoelectron momentum (k) grid, and removal of a smooth background with a series of three cubic splines. E_0 was defined as the energy corresponding to the midpoint of the main absorption step. The resulting oscillations were weighted with k^3 factors and Fourier filtered to isolate first-shell contributions as amplitude and phase functions. Quantitative comparisons between the unknowns and standard, Ni^{II}OEP, were accomplished with nonlinear least square fits based on the EXAFS equation.[32,33]

Results and Discussion

Nonplanar Conformation. The nickel derivatives of porphyrins **3**−**6** have been characterized by NMR, UV−visible absorption, and resonance Raman spectroscopy and other methods. Steric crowding of the peripheral substituents causes the porphyrin macrocycle to deviate from planarity, decreasing the aromatic character. The decreased aromaticity causes NMR upfield shifts in the proton resonances, as a result of diminished ring current effects.[34] For **Ni3**, **Ni4**, **Ni5**, and **Ni6**, upfield shifts are noted for the phenyl and the β-methylene protons relative to nickel derivatives of more planar porphyrins like uroporphyrin (UroP), tetraphenylporphyrin (TPP), and OEP. For example, the β-methylene protons of the acetic acid groups exhibit the largest upfield shift of 1.9 ppm: 5.0 ppm in NiUroP and 3.1 ppm in **Ni4** (each in 0.1 M NaOH/D_2O). A similar shift of 1.8 ppm is observed for the methylene protons in NiOEP and NiOETPP (**Ni2**), which are at 4.1 and 2.3 ppm (at coalescence) respectively.[2a,34]

Recent NMR results for OETPPs have shown that the highly nonplanar macrocycle in solution undergoes a dynamic process of macrocycle inversion (the interconversion between nonplanar conformations).[2,3] This interconversion was monitored by following the temperature dependence of the β-methylene proton resonances. The methylene protons of **Ni3** show a slightly broad singlet at 293 K, indicating fast interconversion. This singlet broadens further and finally appears as an AB doublet upon cooling, indicating inequivalency of the protons. The coupling constant, J_{AB} = 17 Hz, is typical for geminal protons and indicates slow inversion of the saddle conformation on the NMR time scale. The coalescence temperature for the methylene protons of **Ni2** is 293 K, whereas for **Ni3** and **Ni6**, it is 245 and 265 K, respectively. The corresponding free energy of activation, ΔG^* for **Ni2** and **Ni3** is 13.2 and 12.0 kcal mol^{-1}, respectively. The high barrier for NiOETPP could be explained if repulsion among the peripheral substituents is greater for NiOETPP than for the NiOAATPPs. If this were the case, we would also expect NiOETPP to be more nonplanar than NiOAATPP-OME and NiOAATNPP-OME. However, based upon the size of the substituents alone, we would expect the opposite.

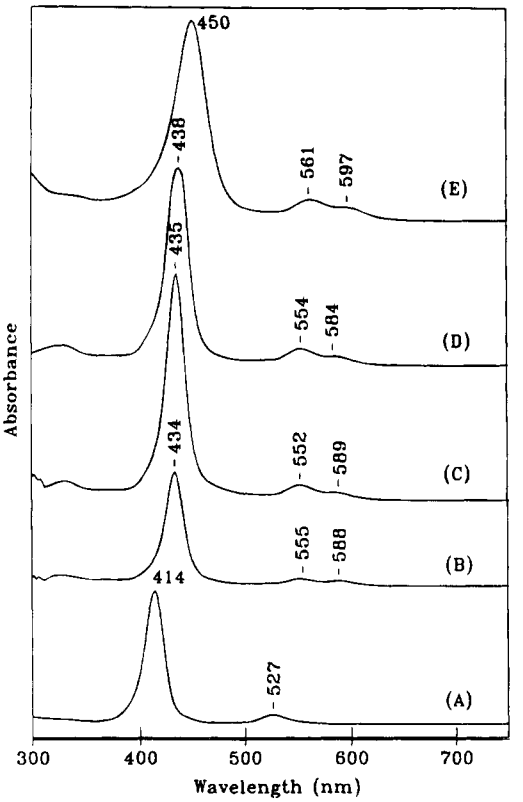

Figure 2. UV−visible absorption spectra of four-coordinate (A) NiTPP, (B) NiOHETPP (**Ni5**), (C) NiOAATPP (**Ni4**), (D) NiOAATPP-OME (**Ni3**), and (E) NiOAATNPP-OME (**Ni6**). Spectra of (1−5) × 10^{-4} M solutions were obtained in either neat methylene chloride or acetone. Baselines in the individual spectra have been arbitrarily shifted for clarity.

The nonplanar conformation of the macrocycle of the NiOATPPs can also be inferred from the optical absorption spectrum. The Soret and the Q absorption bands are red-shifted in nonplanar porphyrins when compared with planar porphyrins.[2,3] The UV−visible absorption spectra of NiTPP, NiOHETPP (**Ni5**), NiOAATPP (**Ni4**), NiOAATPP-OME (**Ni3**) and NiOAATNPP-OME (**Ni6**) in noncoordinating solvents are shown in Figure 2. We observe 19−36-nm red shifts for porphyrins **Ni3**−**Ni6** with respect to NiTPP, a nearly planar porphyrin. Wavelengths of the absorption bands (λ_{max}) for this series of nickel porphyrins are listed in Table 1. The red shifts observed for the NiOAATPPs are comparable to those observed for porphyrins like NiOETPP that are known from the X-ray crystal structure to be highly nonplanar.[35] For the six-coordinate complexes (**Ni3** and **Ni6**) that are formed in 1-methylimidazole (1-MeIm), a red shift with respect to six-coordinate NiTPP is also observed (see Table 1 and Figure 3). The absorption spectrum of the 1-MeIm complex of **Ni6** looks like the spectrum

(31) Furenlid, L. R.; Renner, M. W.; Fajer, J. *Rev. Sci. Instrum.* **1990**, *61*, 1326.
(32) Teo, B. K. *EXAFS: Basic Principles and Data Analysis*; Springer-Verlag: Berlin, Heidelberg, 1986.
(33) Stern, E. A.; Heald, S. M. In *Handbook on Synchrotron Radiation*; Koch, E. E., Ed.; North Holland: Amsterdam, 1983.
(34) Janson, T. R.; Katz, J. J. In *The Porphyrins*; Dolphin, D., Ed.; Academic Press: New York, 1973; Vol. IV, pp 1−59.
(35) Barkigia, K. M.; Renner, M. W.; Furenlid, L. R.; Medforth, C. J.; Smith, K. M.; Fajer, J. *J. Am. Chem. Soc.* **1993**, *115*, 3627−3635.

Table 1. Wavelengths of Absorption Maxima (nm) of Nickel(II) Porphyrins in Various Coordinating and Noncoordinating Solvents

	water			CH_2Cl_2			1-methylimidazole			piperidine		
Ni porphyrin	γ	β	α	γ	β	α	γ	β	α	γ	β	α
NiUroP												
(4-coord)	394	518	552									
+ NaCl	388	518	554									
NiOEP												
(4-coord)	not soluble			391	517	551	392	514	550	396		552
(6-coord)							418			419	542	574
NiTPP												
(4-coord)	not soluble			414	527		418			414	519	
(6-coord)							436	565	609	433	561	600
NiOETPP (**Ni2**)												
(4-coord)	not soluble			433	552	586	434	552	588	435	553	590
NiOHETPP (**Ni5**)												
(4-coord)	not soluble			434[a]	555[a]	588[a]	436	553	586	438	554	592
NiOAATPP (**Ni4**)												
(4-coord)	431	549	587	435[a]	552[a]	589[a]	439	553	588	440	556	589
+ NaCl	431	550	587									
NiOAATPP-OME (**Ni3**)												
(4-coord)	not soluble			438	554	584	438	554	584	440		
(6-coord)							458			464		693
NiOAATNPP-OME (**Ni6**)												
(4-coord)	not soluble			450	561	597						
(6-coord)							476		704	489		717

[a] Spectra obtained in acetone. In CH_2Cl_2 and acetone, most Ni(II) porphyrins listed here give similar absorption spectra.

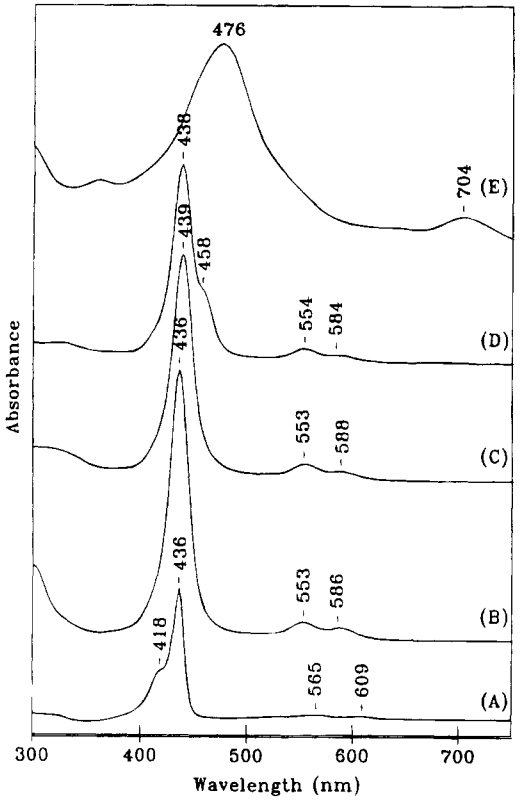

Figure 3. UV−visible absorption spectra of (A) NiTPP, (B) NiOHETPP (**Ni5**), (C) NiOAATPP (**Ni4**), (D) NiOAATPP-OME (**Ni3**), and (E) NiOAATNPP-OME (**Ni6**) in coordinating solvent. Spectra of (1−5) × 10^{-4} M solutions were obtained in 1-methylimidazole. Baselines in the individual spectra have been arbitrarily shifted for clarity.

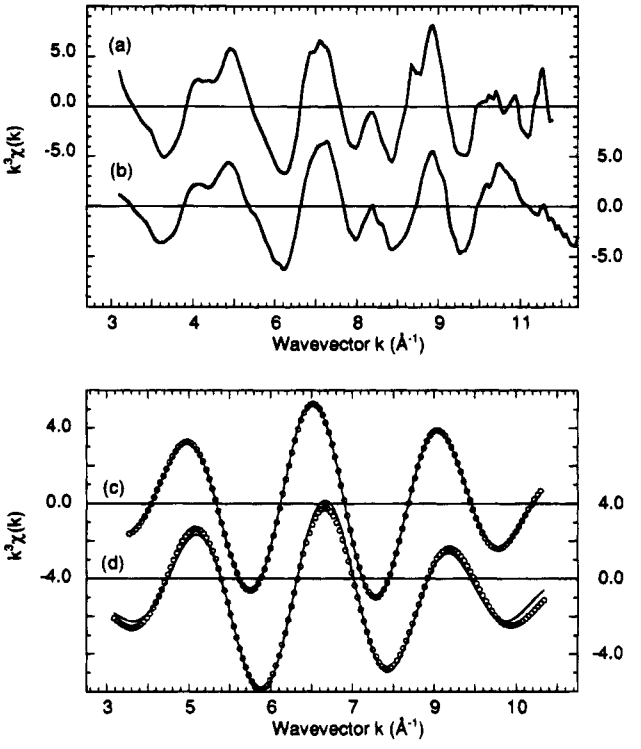

Figure 4. The k^3 weighted EXAFS data for (a) **Ni3** and (b) **Ni6**. The isolated first-shell EXAFS oscillations (—) and nonlinear least-squares fits (○) for (c) **Ni3** and (d) **Ni6**.

of the dication (**$H_4$6**). However, demetalation has not occurred because evaporation of the coordinating solvent followed by dissolution in noncoordinating solvents gives the normal four-coordinate absorption spectrum of the metal derivative. Apparently, the nitro groups of **Ni6** are electronically coupled to the macrocycle $\pi-\pi^*$ transitions. The coupling is evident from position of the Soret band in methylene chloride, which is red-shifted by an additional 12 nm compared to that of **Ni3**, and from the very large red shift of the Soret band of six-coordinate **Ni6**, relative to other nonplanar six-coordinate Ni porphyrins.

EXAFS studies support the conclusion that **Ni3** and **Ni6** have highly nonplanar conformations. See Figure 4 and Table 2. (Figures showing the absorption edges and Fourier-transformed EXAFS data are included in the supplementary material.) The presence and intensity of the $1s-4p_z$ pre-edge peak in both **Ni3** and **Ni6** clearly show four-coordinate and square-planar environments for the nickel. The k^3 weighted EXAFS spectra for **Ni3** and **Ni6** are shown in Figure 4, traces a and b, respectively. The isolated first shell EXAFS oscillations and the nonlinear least-square fits are shown in Figure 4, traces c and d. Analysis

Table 2. EXAFS Results[a] for Nickel Complexes at 300 K

complex	N	r, Å (±0.01)	$\Delta\sigma^2$ (±0.001)	χ^2 gof
NiOAATPP-OME[b]	3.57	1.92	−0.001	0.003
NiOAATNPP-OME[c]	4.11	1.89	0.002	0.067
NiOETPP[d]	3.57	1.91	0.001	0.002

[a] N is the coordination number per nickel. The nickel coordinating atom distance (r) is determined from fits of the first-shell EXAFS data. $\Delta\sigma^2$ is a relative mean square deviation in r (the square of the Debye–Waller factor), $\Delta\sigma^2 = \sigma^2$ unknown $- \sigma^2_{std}(Ni^{II}OEP)$. χ^2 gof is a relative goodness-of-fit statistic, defined as $\sum(\text{exp} - \text{fit})^2/\sum\text{exp}^2$. Experimental details: k range ~3.3–10.5, Hanning window 0.5 Å^{-1}, weighting k^3, R window ~0.8–2.2 Å, Hanning window ~0.1 Å. [b] Measured in 2-methyltetrahydrofuran. [c] Measured as a solid. [d] Measured in tetrahydrofuran (ref 35).

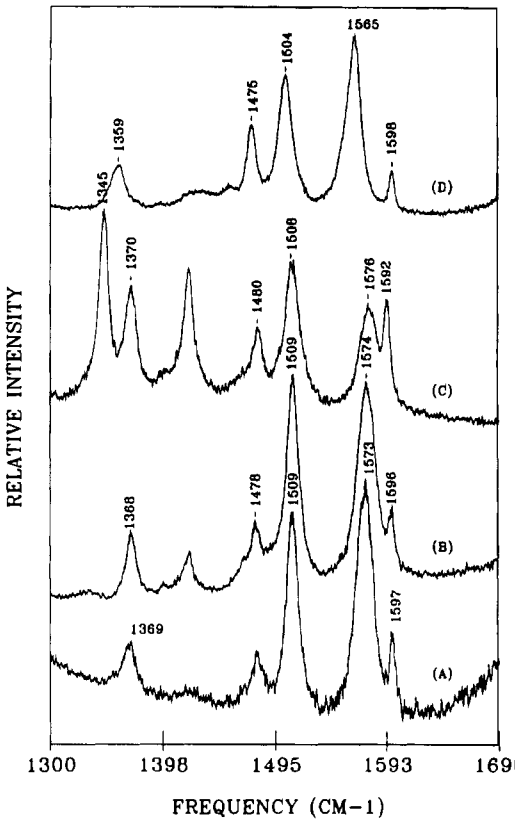

Figure 5. Resonance Raman spectra of (A) NiOAATPP, (B) NiOAATPP-OME, (C) NiOAATNPP-OME, and (D) NiOHETPP. Solvent for porphyrin solution was either methylene chloride or acetone, and 413.1-nm laser excitation was used for obtaining Raman spectra.

of the EXAFS data yields average Ni–Ni distances of 1.92(2) and 1.89(2) Å for **Ni3** and **Ni6**, respectively. These short Ni–N distances are comparable to those found in **Ni2** (1.906 ± 0.002 and 1.91 Å, from the crystal structure and EXAFS measurements, respectively) for which the crystal structure shows a saddle-shaped macrocycle conformation.[35] No planar nickel porphyrins have such short Ni–N distances. The possibly shorter bond length in **Ni6** relative to **Ni3**, porphyrins differing only in the substitution of a nitro group at the phenyl para position, suggests either increased nonplanarity or increased electron depletion at the macrocycle caused by the nitro substituent (*vide infra*).

Resonance Raman spectra for the nickel complexes of OAATPP, OAATPP-OME, OAATNPP-OME and OHETPP are shown in Figure 5, and the frequencies of some structure-sensitive porphyrin modes and a phenyl mode are listed in Table 3. An additional spectral feature is observed for the nitrophenyl derivative; the Raman line at 1345 cm^{-1} in spectrum C of Figure 5 most likely is the symmetric stretch of the nitro groups at the

Table 3. Resonance Raman Frequencies (cm^{-1}) of Structure-Sensitive Marker Lines for Ni(II) Porphyrins in Noncoordinating Solvents and under Various Aqueous Conditions

nickel porphyrin/solvent	ν_4	ν_3	ν_2	ν_ϕ
OEP/CH_2Cl_2	1383	1519	1600	
TPP/CH_2Cl_2	1374	1470[a]	1572	1600
OETPP (**Ni2**)/CH_2Cl_2	1360	1504	1562	1597
OHETPP (**Ni5**)/acetone	1359	1504	1565	1598
OAATPP-OME (**Ni3**)/CH_2Cl_2	1368	1509	1574	1596
OAATNPP-OME (**Ni6**)/CH_2Cl_2	1370	1508	1576	1592
OAATPP (**Ni4**)/acetone[b]	1369	1509	1573	1597
H_2O/pH 3[b]	1370	1511	1577	1596
H_2O/pH 7[b]	1368	1510	1569	1599
H_2O/pH 13[b]	1367	1509	1568	1598
H_2O/pH 13/NaCl[b]	1367	1509	1567	1598

[a] The potential energy distribution of this mode is radically altered for TPP as compared to OEP and OETPP, based on normal coordinate analyses for NiTPP and NiOEP given in ref 30. [b] $\sum\sigma_m$ values are estimated to be between 0.00 and −0.32 depending on the degree of ionization of the eight acid substituents.

para positions of the meso-phenyl groups.[13,15] The 1345-cm^{-1} Raman line of OAATNPP-OME is more enhanced (with respect to ν_4) for laser excitation at 458 nm near the Soret than at 413 nm, possibly suggesting that porphyrin–NO_2 charge-transfer transitions are coupled to the π–π^* transitions.

Generally, nonplanar distortions of the porphyrin macrocycle cause large downshifts in the structure-sensitive Raman marker lines when compared to similar spectra of a planar nickel porphyrin.[2,3] The relative sizes of the downshifts within a series of porphyrins can generally be used as a measure of the degree of macrocyclic distortion.[13,36,37] In particular, ν_4, ν_3, and ν_2 all downshift by 15–43 cm^{-1} for the distorted octaethyl- or octapropyltetraphenylporphyrins relative to planar NiOEP.[36,37] For the series of NiOAATPP derivatives investigated here, these lines downshift by 8–35 cm^{-1} relative to NiOEP, and therefore, these derivatives must be nearly as highly distorted as NiOETPP. However, the NiOAATPP derivatives vary considerably in the electron-withdrawing properties of the substituents, and thus an electronic effect on the Raman frequencies is also expected.

To accurately interpret the frequency differences within this group of NiOAATPPs, it is important first to compare only porphyrins with similar electronic properties to determine the effect of structural differences. The deprotonated acetate and hydroxyethyl moieties of **Ni4** and **Ni5**, respectively, have electronic properties (σ_m) that are the same as those of the ethyls of **Ni2**. As expected, **Ni2** and **Ni5** have almost identical Raman frequencies (Figure 5 and Table 3); however, **Ni4** has significantly higher frequencies for the structure-sensitive marker lines. The nearly identical Raman frequencies for **Ni2** and **Ni5** can be attributed to the similarities in both the steric and electronic properties of the substituents. On the other hand, the acetate groups of **Ni4** (pH >7) are more bulky and would be expected to sterically induce larger distortions from planarity than observed for **Ni2**, resulting in significantly *lower* frequencies than **Ni2**. Instead, the observed *higher* frequencies indicate some other structural perturbation that is not associated with either the steric properties or the electron-withdrawing/donating properties of the substituents. Intra- and intermolecular hydrogen bonding provide possible additional perturbations for the acetate groups of **Ni4**.

Electronic Effects. The subtle frequency differences in the structure-sensitive Raman lines within the series of NiOAATPPs

(36) Shelnutt, J. A.; Majumder, S. A.; Sparks, L. D.; Hobbs, J. D.; Medforth, C. J.; Senge, M. O.; Smith, K. M.; Miura, M.; Luo, L.; Quirke, J. M. E. *J. Raman Spectrosc.* **1992**, *23*, 523.
(37) Sparks, L. D.; Anderson, K. K.; Medforth, C. J.; Smith, K. M.; Shelnutt, J. A. *Inorg. Chem.* **1994**, *33*, 2297.

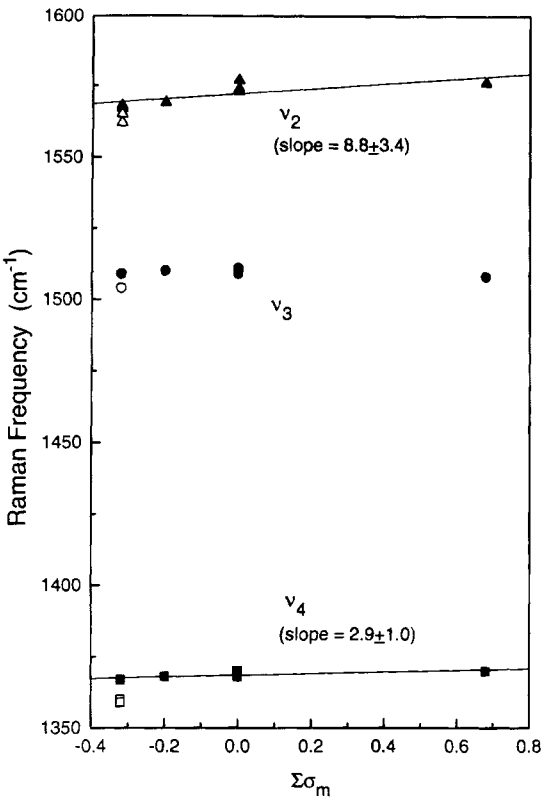

Figure 6. Linear relationships between the frequencies of the Raman lines ν_4, ν_3, and ν_2 for the nickel porphyrins listed in Table 2 and the electron-withdrawing properties of the peripheral substituents as measured by $\Sigma\sigma_m$ given in Table 3: nickel octaacid tetraphenylporphyrins (solid symbols); NiOETPP and NiOHETPP (open symbols). Slopes of the lines and standard deviations are given in parentheses. The slopes are, within error, the same as for the FeDPPF$_x$ series, except for ν_4, which has a significantly smaller slope for the nickel octaacid tetraphenylporphyrins.

(**Ni3**, **Ni4**, **Ni6**) can be interpreted in terms of differences in the electronic effects of the peripheral substituents. A similar dependence of the position of the absorption bands on electron-withdrawing properties of the substituents is already known for another series of porphyrins.[38] Table 3 lists the sum of the Hammett constants[39] ($\Sigma\sigma_m$), a measure of the electron-withdrawing/donating ability of the chemical moieties substituted on each porphyrin of the series, and these $\Sigma\sigma_m$ values can be used to estimate the inductive electronic effect. Almost identical conformations are expected on the basis of the peripheral crowding, so that the electronic effect is clearly evident in this series. For example, NiOAATPP-OME and NiOAATNPP-OME should exhibit almost identical conformations because the *p*-NO_2 groups on the phenyls do not significantly increase the steric crowding. Thus, the 2-cm^{-1} increases in frequency noted for ν_4 and ν_2 are most likely a result of the larger electron-withdrawing effect of the nitrophenyl groups compared to the phenyls. In fact, the frequencies of ν_4 and ν_2 for the entire series of NiOAATPP derivatives show fair correlations with $\Sigma\sigma_m$ as illustrated in Figure 6. (NiOETPP and NiOHETPP clearly exhibit unusually low frequencies relative to this linear relationship because of structural effects and for this reason were not included in the linear regressions.)

Similar dependence of ν_4 and ν_2 on the electron-withdrawing capacity of substituents has been observed for other conformationally homologous series of porphyrins, including a series of fluorinated tetraphenylporphyrins (TPPF$_x$, x = 0, 20) and dodecaphenylporphyrins (DPPF$_x$, x = 0, 20, 28, 36).[40] In both the Fe^{III}- and Ni^{II}DPPF$_x$ series, ν_4 and ν_2 (but not ν_3) increase in proportion to the number of fluorines and to $\Sigma\sigma_m$. Further, molecular mechanics calculations, which neglect any electronic effect of the substituents, indicate no significant structural differences among the NiDPPF$_x$ series, suggesting that the changes are entirely a result of the electron-withdrawing effect of the fluorines. Comparable shifts in ν_4 and ν_2 are also observed for the planar porphyrins NiTPP and NiTPPF$_{20}$, thus these shifts cannot be attributed to a change in nonplanar distortion. The increases in Raman frequency with unit increase in $\Sigma\sigma_m$ for the NiOAATPP series reported here (slopes given in Figure 6) are similar to the slopes for the DPPF$_x$ and TPPF$_x$ series, supporting the assertion that the electronic effect is the largest contributor to the shifts for the NiOAATPP series.

One can ask whether the electron-withdrawing effect of the substituents actually causes a conformational change and whether it is this nonsteric structural change that is measured by the shifts in the Raman lines. A possible interpretation is that the core size contracts for the more electron-withdrawing substituents. Core contraction causes an increase in the marker line frequencies for planar and nonplanar porphyrins.[2,37]

In summary, while the shifts observed for the octaacid porphyrins are, in part, due to the electron-withdrawing/donating effect of the substituents, variations resulting from structural changes are also evident. From Figure 6, the data further suggest that the higher frequencies of ν_4, ν_3, and ν_2 for most of the porphyrins (**Ni4**, **Ni3**, and probably **Ni6**) relative to **Ni2** and **Ni5** result in part from the more nonplanar conformation of the latter porphyrins. In addition, a more planar conformation for both **Ni3** and **Ni6** also accounts for their lower barriers to inversion (compared to **Ni2**) given by the NMR measurements.

Axial Coordination. The affinity for axial coordination of nitrogenous ligands is also thought to be affected both by electron-withdrawing substituents and by nonplanarity of the macrocycle.[3a,13] Planar porphyrins such as NiOEP and NiTPP readily bind nitrogenous ligands, whereas nonplanar NiOETPP does not and remains four-coordinate, even though its $\Sigma\sigma_m$ (−0.32) lies between NiOEP (−0.56) and NiTPP (0.24). Also, the NiOAATPP series of nonplanar porphyrins shows increased ligand affinity with increased electron-withdrawing capacity of the peripheral groups. Table 4 shows a direct correlation between the overall electron-withdrawing capacity of the substituents for nonplanar porphyrins ($\Sigma\sigma_m$) and the relative binding of 1-MeIm in the neat solvent. Similar trends in ligand affinity are also observed for pyridine and piperidine. More electron-withdrawing peripheral substituents may enhance the electron deficiency of the metal, leaving the nickel ion even

Table 4. Sum of Hammett σ Values, $\Sigma\sigma_m$, of Different Nickel Porphyrins and Their Relative Binding to 1-Methylimidazole at Room Temperature

nickel porphyrin	$\Sigma\sigma_m$	% bound
OEP	−0.56	5
OETPP (**Ni2**)	−0.32	0
OHETPP (**Ni5**)	−0.32	0
OAATPP (deprotonated)[a] (**Ni4**)	−0.32	0
OAATPP-OME (**Ni3**)	0.00	25
TPP	0.24	70
OAATNPP-OME (**Ni6**)	0.68	100

[a] $\Sigma\sigma_m$ values are estimated to be between 0.00 and −0.32 depending on the degree of ionization of the eight acid substituents.

(38) Meot-Ner, M.; Adler, A. D. *J. Am. Chem. Soc.* **1975**, *97*, 5107.
(39) Hausch, C.; Leo, A. *Substituent Constants for Correlation Analysis in Chemistry and Biology*; John Wiley & Sons: New York, 1979.
(40) Anderson, K. K.; Majumder, S. A.; Hobbs, J. D.; Sparks, L. D.; Medforth, C. J.; Forsyth, T. P.; Smith, K. M.; Shelnutt, J. A. Unpublished results.

less coordinatively saturated and increasing the axial ligand affinity. The failure of NiOAATPP to bind 1-MeIm may be due to deprotonation of the acid groups in this solvent, making the acid groups more electron donating (the pK_a values for imidazole and the acetic acid groups are 7.0[41] and 6.5,[20] respectively).

Aggregation. We have also examined the aggregation behavior of NiOAATPP in aqueous environments and compared it with that of planar NiUroP. NiUroP shows no evidence of aggregation in basic solutions, but upon addition of salt (>1 M) or acid (pH <6), $\pi-\pi$ aggregates are formed.[20] Aggregation of NiUroP is caused by shielding of the −8 charge of the deprotonated acid groups and results in a large blue shift in the Soret absorption band (see absorption spectra in supplementary Figure S3, A and B). The Soret absorption band (γ) of the MUroP aggregate exhibits marked broadening and a blue shift of 10−15 nm (depending on the metal derivative) with respect to the Soret band of the corresponding monomer. The α and β bands of MUroP aggregates are also broadened but red-shift to a lesser extent. For the resonance Raman spectra, the $\pi-\pi$ aggregation of NiUroP (for both planar and nonplanar conformers) gives 1−5 cm^{-1} shifts to higher frequency in the structure-sensitive Raman lines.[20,22,23] In contrast with those of NiUroP, the UV−visible spectra of NiOAATPP show no evidence of aggregation under similar solution conditions (see supplementary Figure S3, C and D). Further, the resonance Raman spectra for NiOAATPP (see spectra in supplementary Figure S4 and Table 3) at different pH values and after adding NaCl at high pH show no evidence for aggregation. Structure-sensitive Raman lines shift to lower frequencies at high pH due to the decreased electron-withdrawing capacity of the deprotonated acetic acid groups, but show no indication of shifts characteristic of aggregation.

Summary and Conclusions

The evidence from the NMR, EXAFS, optical absorption and resonance Raman spectroscopies indicate that NiOHETPP and NiOAATPP and the latter's derivatives have highly nonplanar conformations. The structure-sensitive Raman lines vary depending on the degree of porphyrin nonplanarity and also the inductive electronic effect of the substituents. Within the series of NiOATPPs, the shifts in Raman frequencies correlate with the electron-withdrawing properties of the substituents. Solution NMR studies indicate that the macrocycles are fluxional at room temperature, undergoing interconversion between nonplanar forms that are related by inversion. Temperature dependent NMR studies yield activation barriers of 12−13 kcal mol^{-1}. EXAFS measurements confirm the highly nonplanar conformations of these complexes by the short metal−nitrogen distances. While the Ni−N bond distance and the diminished ring current effects both indicate that NiOAATPP-OME is highly nonplanar, the free energies of activation for macrocycle inversion and the resonance Raman frequencies indicate that the NiOAATPP derivatives are slightly more planar than NiOETPP. The structure-sensitive Raman lines and the optical absorption spectra are found to vary depending on the degree of porphyrin nonplanarity and also the electronic effects of the substituents.

The ligand binding affinity of nickel porphyrins is dependent on both macrocycle conformation and electronic effects. Ni-OAATPP-OME binds axial nitrogenous bases despite having a nonplanar geometry nearly as distorted as NiOETPP (**Ni2**) which remains four-coordinate even in strong bases. Binding occurs because the acetic acid ester substituents are less electron donating than ethyl groups. Among the NiOAATPP derivatives which have similar nonplanar distortions, ligand binding affinity appears to be directly correlated to electron-withdrawing ability of the substituents as estimated from the sum of their Hammett σ_m constants.

The nonplanar conformation of OAATPP prevents the expected $\pi-\pi$ aggregation of planar octaacid porphyrins like UroP. The spectra of NiOAATPP show no evidence of aggregation upon addition of salt (>1 M) or acid (pH <6). In an effort to exploit the unique aggregation properties of the OAATPP derivatives, we recently synthesized a lipoporphyrin with long alkane tails and with NiOAATPP-OME as the polar head group. Using this lipoporphyrin, we have constructed mixed Langmuir−Blodgett films of the lipoporphyrin with stearic acid. These films show no evidence of aggregation of the porphyrin macrocycles or of phase separation from the stearic acid component, which is typical of planar lipoporphyrins.[42]

Acknowledgment. The authors thank Robert A. Rieger and Charles Iden (SUNY, Stony Brook, NY) for mass spectral analyses. Work at Sandia National Laboratories was supported by U.S. Department of Energy (DOE) Contract DE-AC04-94AL85000 (J.A.S.). Work at Brookhaven National Laboratory was performed under the aegis of a DOE/Sandia contract (M.M.) and DOE Contract DE AC02-76CH00016 (M.W.R.). S.A.M. and J.D.H. acknowledge Associated Western Universities fellowships. X-ray absorption data were collected on beam lines X-11A and X-10C of the National Synchrotron Light Source at Brookhaven National Laboratory. X-11A is supported by the Division of Materials Sciences, U.S. Department of Energy, under Contract DE-FG05-89ER4384.

Supplementary Material Available: Figures S1−S4, showing X-ray absorption edges and Fourier transforms of isolated EXAFS oscillations for Ni3 and Ni6 and UV−visible absorption spectra of NiUroP and NiOAATPP under various aqueous solvent conditions (5 pages). This material is contained in many libraries on microfiche, immediately follows this article in the microfilm version of the journal, and can be ordered from the ACS; see any current masthead page for ordering information.

(41) *The Merck Index*, 9th ed.; Merck & Co.: Rahway, NJ, 1976; p 4811.

(42) Song, X.; Miura, M.; Xu, X.; Anderson, K. K.; Majumder, S. A.; Hobbs, J. D.; Cesarano, J.; Shelnutt, J. A. Manuscript in preparation.